Spin–orbit coupling and Jahn–Teller distortion in bimetallic oxalates

Randy S. Fishman *, Satoshi Okamoto, Fernando A. Reboredo

Materials Science and Technology Division, Oak Ridge National Laboratory, P.O. Box 2008, Oak Ridge, Tennessee 37831-6065, United States

ARTICLE INFO

ABSTRACT

The C_3-symmetric crystal-field potential in the Fe(II)Fe(III) bimetallic oxalates splits the $L = 2$ Fe(II) multiplet into two doublets and one singlet. In compounds that exhibit magnetic compensation, one of the doublets lies lowest in energy and carries an average orbital angular momentum L_z^{cf} that exceeds a threshold value of roughly 0.25. In a range of L_z^{cf}, a Jahn–Teller (JT) distortion enhances the splitting of the low-lying doublet and breaks the C_3 symmetry of the bimetallic planes around the ferrimagnetic transition temperature. Due to the competition with the spin-orbit coupling, the JT distortion disappears at low temperatures in compounds that display magnetic compensation. A comparison with recent measurements provides compelling evidence for this inverse, low-temperature JT transition. The size of the JT distortion is estimated using first-principles calculations, which suggest that the long-range ordering of smaller, non-C_3-symmetric organic cations can eliminate magnetic compensation.

© 2008 Elsevier Ltd. All rights reserved.

1. Introduction

A Jahn–Teller (JT) distortion [1] removes the degeneracy of a singly-occupied electronic orbital by an atomic displacement. Because it also mixes the degenerate levels, a JT distortion reduces their average orbital angular momenta $\langle \mathbf{L} \rangle$. By contrast, the spin–orbit coupling $\lambda \mathbf{L} \cdot \mathbf{S}$ favors the largest possible magnitude for $\langle \mathbf{L} \rangle$. So a JT distortion is prevented when the spin–orbit coupling is sufficiently strong. Consequently, the most common JT distortions involve Mn(III) ions in octahedral crystal fields, which quench the average orbital angular momentum of the degenerate e_g levels [2]. Several recent studies of molecule-based magnets [3] have reported JT distortions involving Mn(III) ions with quenched orbital angular momentum.

When the spin–orbit coupling and JT energies are comparable, however, the orbital angular momentum may not be quenched and a pseudo-JT distortion with rather interesting behavior is possible. In this paper, we study the JT distortion in the bimetallic oxalates, which are a class of molecule-based magnets where the average orbital angular momentum of the degenerate electronic levels can be modified by choosing different organic cations to lie between the bimetallic layers. Due to the strong orbital ordering of Fe(II) ions at low temperatures, a JT distortion may only appear at intermediate temperatures around the transition temperature T_c. The JT distortion of the Fe(II) ions then vanishes below a lower critical temperature with the reappearance of the undistorted phase at low temperatures. The bimetallic oxalates may provide the first example of such an inverse JT transition.

One of the most intensively-studied classes of molecule-based magnets, bimetallic oxalates A[M(II)M′(III)(ox)₃] were first synthesized [4] in 1992. On the open honeycomb lattice of each bimetallic layer, sketched in Fig. 1a, the transition-metal ions M(II) and M′(III) are coupled by the oxalate bridges ox = C_2O_4 [5]. Depending on the metal atoms, a single bimetallic layer can be either ferromagnetic or ferrimagnetic (M(II) and M′(III) spins parallel or anti-parallel) with magnetic moments pointing out of the plane. While the organic cation A separating the layers cannot reverse the sign of the exchange coupling, it can change the overall properties of the system.

Several Fe(II)Fe(III) bimetallic oxalates exhibit magnetic compensation (MC) due to the cancellation of the moments on the Fe(II) and Fe(III) sublattices below the ferrimagnetic transition temperature T_c [6,7]. Based on symmetry and energy considerations, we recently explained why MC occurs for some organic cations but not for others [8]. The C_3-symmetric crystal field (invariant under in-plane rotations of $2\pi/3$) splits the $L = 2$ Fe(II) multiplet into two doublets and a singlet. By shifting the Fe(II) ions with respect to the oxalate molecules, the cation A determines the average orbital angular momentum L_z^{cf} carried by the low-energy doublet, which is then split by the spin–orbit coupling. Fe(II)Fe(III) compounds exhibit MC when the low-energy doublet lies below the singlet and L_z^{cf} exceeds the threshold $l_c \approx 0.25$. For compounds that do not exhibit MC (so called "normal" compounds), either $L_z^{cf} < l_c$ or the singlet level lies lowest in energy.

In the absence of spin–orbit coupling or when $L_z^{cf} = 0$, a JT distortion that violates C_3 symmetry will always split the low-energy doublet. For large enough L_z^{cf}, the spin–orbit coupling will eliminate the JT distortion. However, in a range of L_z^{cf} that includes l_c, a JT-distorted phase appears between temperatures $T_{JT}^{(l)}$ and $T_{JT}^{(u)}$

* Corresponding author. Tel.: +1 865 579 6855; fax: +1 865 574 4913.
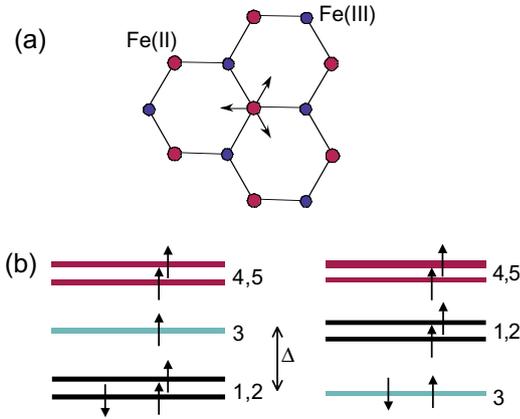*E-mail address:* fishmanrs@ornl.gov (R.S. Fishman).

Fig. 1. (a) A portion of the open honeycomb lattice, displaying three equivalent displacements of the Fe(II) ion into the adjacent hexagons. (b) Two possible level-splitting schemes of the $3d^6$ Fe(II) orbitals in a C_3-symmetric crystal-field, with either the doublet $\psi_{1,2}$ or the singlet ψ_3 lowest in energy.

that bracket T_c [9]. Both the inverse, low-temperature transition $T_{JT}^{(l)}$ and the normal, high-temperature transition $T_{JT}^{(u)}$ are first order or discontinuous when the elastic parameters are appropriately chosen. A comparison with recent experiments [10] allows us to estimate the normal JT transition temperature $T_{JT}^{(u)}$ for Fe(II)Fe(III) bimetallic oxalates that exhibit MC. For normal Fe(II)Fe(III) compounds, the JT distortion either persists down to $T = 0$ if the doublet lies below the singlet or is absent altogether if the singlet lies below the doublets.

This paper contains an extended description of the JT transition first discussed in Ref. [9]. Section 2 develops the phenomenological model for MC and the JT distortion, with results discussed in Section 3. First-principles calculations are described in Section 4 and a summary is presented in Section 5.

2. Model

Bimetallic oxalates are characterized by three energy scales. The dominant energy is the Hund's coupling that determines the spins $S = 2$ and $S' = 5/2$ on the Fe(II) ($3d^6$) and Fe(III) ($3d^5$) sites. Next in importance is the C_3-symmetric crystal field V generated by the 6 oxygen atoms around each of the Fe sites. These 6 oxygen atoms form two triangles of slightly different sizes rotated by about 48° with respect to each other, one above and the other below the plane of Fe atoms. Because the two triangles have different sizes, the six oxygen atoms do not span a trigonally-compressed octahedron [11] and C_3 symmetry is the only point-group symmetry obeyed by the crystal-field potential. The weakest energies are the antiferromagnetic exchange coupling $J_c \mathbf{S}_i \cdot \mathbf{S}'_j$ between the Fe(II) and Fe(III) moments within each bimetallic layer, the spin–orbit coupling $\lambda \mathbf{L}_i \cdot \mathbf{S}_i$ on the Fe(II) sites ($\lambda \approx -12.65$ meV [12]), and any non-C_3-symmetric contributions of the crystal potential.

As shown in Fig. 1b, the C_3-symmetric potential V splits the $L = 2$ multiplet of the Fe(II) sites into two doublets $\psi_{1,2}$ and $\psi_{4,5}$, and a singlet ψ_3. We demonstrated in Ref. [8b] that the low-energy doublet $\psi_{1,2}$ carries an average orbital angular momentum $L_z^{cf} = |\langle \psi_{1,2}|L_{iz}|\psi_{1,2}\rangle|$ between 0 and 2, depending on the crystal-field parameters. Of course, the singlet state ψ_3 does not carry any orbital angular momentum.

Keep in mind that the orbital angular momenta L_z^{cf} of the low-energy doublet is modified by the crystal fields. It is not the same as the total angular momenta L of the Fe(II) multiplet before the crystal field is taken into account. Because $\langle \psi_{1,2}|\mathbf{L}_i|\psi_{1,2}\rangle = \pm L_z^{cf}\mathbf{z}$, the average orbital angular momentum of the doublet is an Ising-like degree of freedom.

So the effective Hamiltonian of the Fe(II)Fe(III) bimetallic oxalates is given by

$$H = J_c \sum_{\langle i,j\rangle} \mathbf{S}_i \cdot \mathbf{S}'_j - |\lambda| \sum_i S_i^z L_i^z, \tag{1}$$

where the $\langle i,j\rangle$ sum runs over all nearest-neighbors and the i sum runs over all Fe(II) sites. The antiferromagnetic exchange J_c is positive. As discussed above, $L_i^z = \pm L_z^{cf}$. This model has recently been generalized [13] to treat any bimetallic oxalate, with possible spin–orbit coupling on both the M(II) and M′(III) sites.

Including its orbital contribution, the Fe(II) magnetic moment can be written $M(T) = M_S(T) + M_L(T) \leqslant 0$, where $M_S = 2\langle S_i^z\rangle$ and $M_L = \langle L_i^z\rangle$. The Fe(III) magnetic moment $M'(T) = M_{S'}(T) = 2\langle S_j^z\rangle \geqslant 0$ contains no orbital contribution. Mean-field (MF) theory is used to treat the nearest-neighbor exchange

$$J_c \mathbf{S}_i \cdot \mathbf{S}'_j \approx J_c\left\{\left(M_S S_j^{z'} + S_i^z M_{S'}\right)/2 - M_S M_{S'}/4\right\} \tag{2}$$

between neighboring Fe(II) and Fe(III) spins. The MF eigenvalues of $\psi_{1,2;\sigma}$ and $\psi_{3\sigma}$ with z spin component $\sigma = 0, \pm 1$ or ± 2 are

$$\epsilon_{1\sigma} = (-|\lambda|L_z^{cf} + 3J_c M_{S'}/2)\sigma, \tag{3}$$

$$\epsilon_{2\sigma} = (|\lambda|L_z^{cf} + 3J_c M_{S'}/2)\sigma, \tag{4}$$

$$\epsilon_{3\sigma} = (3J_c M_{S'}/2)\sigma + \Delta, \tag{5}$$

so that the doublet $\psi_{1,2;\sigma}$ is split by the spin–orbit coupling with $|\epsilon_{2\sigma} - \epsilon_{1\sigma}| = 2|\lambda\sigma|L_z^{cf}$. Because the crystal-field potential is assumed much larger than the spin–orbit and exchange energies, $|\Delta| \gg J_c$ or $|\lambda|$.

Using Eqs. (3) and (4) for the eigenvalues $\epsilon_{1,2;\sigma}$, it is straightforward to evaluate $M(T), M'(T)$, and the average magnetization $M^{avg}(T) = (M(T) + M'(T))/2 = (|M'(T)| - |M(T)|)/2$. When $l_c \approx 0.238 < L_z^{cf} < 1$, $M^{avg}(T)$ passes through 0 at the compensation temperature $T_{comp} < T_c$. Just below T_c, $M^{avg}(T) < 0$ because the parallel spin–orbit coupling between $\mathbf{L}_i$ and $\mathbf{S}_i$ causes the Fe(II) moment $M(T)$ to increase in amplitude more rapidly than the Fe(III) moment $M'(T)$. But at $T = 0$, the Fe(III) moment saturates at the larger value $|M'(0)| = 2S' > |M(0)| = 2S + L_z^{cf}$ so that $M^{avg}(0) > 0$.

After comparing the observed values of $T_{comp}/T_c \approx 0.62$ and $T_c \approx 45$ K with the theoretical predictions, we estimated [8] that $J_c \approx 0.46$ meV and $L_z^{cf} \approx 0.28$ in MC compounds. Normal compounds can fall into two categories. Either the doublet remains lower than the singlet ($\Delta > 0$) but with $L_z^{cf} < l_c' \approx 0.234$ or the singlet lies lowest in energy ($\Delta < 0$). Our model also predicted that two compensation points were possible in the narrow window $l_c' < L_z^{cf} < l_c$. The recent observation by Tang et al. [10] of two compensation points in the compound N(n-C$_4$H$_9$)$_4$[Fe(II)Fe(III)ox$_3$] (data shown in the inset to Fig. 2a) would seem to confirm that prediction.

In the absence of spin–orbit coupling, a doubly-degenerate level occupied by a single electron is always split by a local displacement of the ion, which linearly lowers the electronic energy while incurring a quadratic cost in the elastic energy. The mixing of the Fe(II) eigenstates $\psi_{1\sigma}$ and $\psi_{2\sigma}$ due to the JT distortion is described by the Hamiltonian[1]

$$\underline{H}_\sigma^{mix} = \begin{pmatrix} \epsilon_{1\sigma} & \xi \\ \xi & \epsilon_{2\sigma} \end{pmatrix}, \tag{6}$$

where ξ is independent of σ. If $\epsilon_{1\sigma} = \epsilon_{2\sigma}$ are given by the MF result $\epsilon_{0\sigma} \equiv 3J_c M'\sigma/2$, then the eigenstates of $\underline{H}_\sigma^{mix}$ are

---

[1] Diagonal terms in $\underline{H}_\sigma^{mix}$ involving ξ can be neglected because the doublet states are related by the time-reversal operations $\psi_{1\sigma} = -K\psi_{2,-\sigma}$ and $\psi_{2\sigma} = -K\psi_{1,-\sigma}$, where K is the time-reversal operator. So for any spin-independent electrostatic potential $V = K^{-1}VK$, $\langle \psi_{1\sigma}|V|\psi_{1\sigma}\rangle = \langle \psi_{2,-\sigma}|K^{-1}VK|\psi_{2,-\sigma}\rangle = \langle \psi_{2\sigma}|V|\psi_{2\sigma}\rangle$, leading only to a shift of the doublet with respect to the singlet.
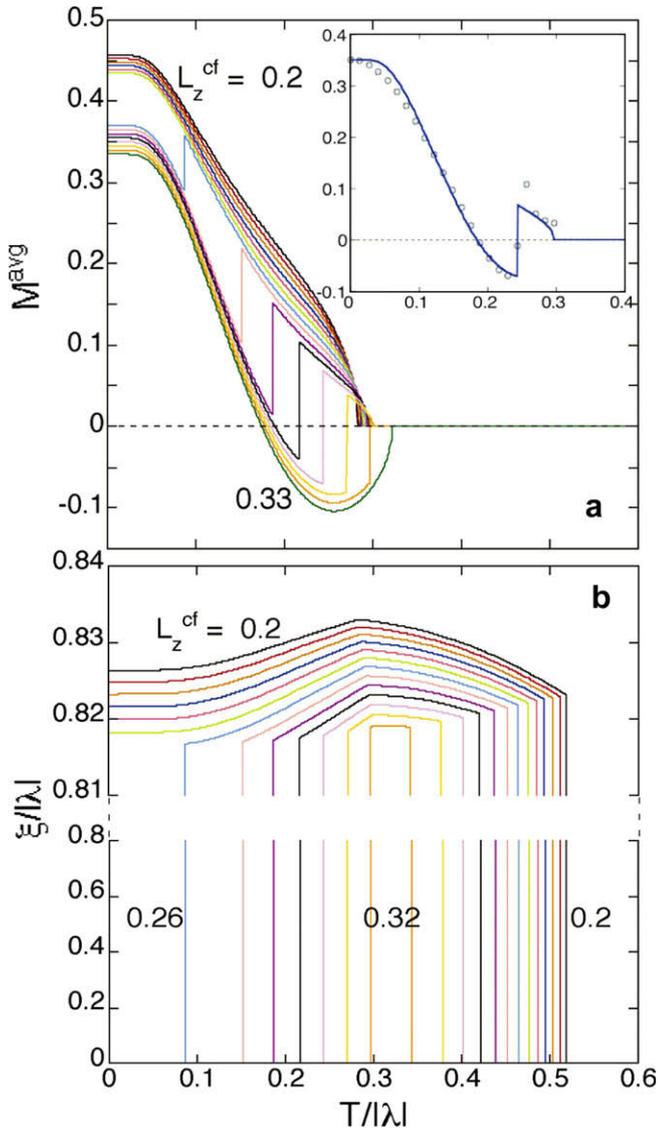
Fig. 2. (a) The average magnetization and (b) the JT energy ξ normalized by $|\lambda|$ versus temperature $T/|\lambda|$ for a range of L_z^{cf} in increments of 0.01 using $J_c/|\lambda| = 0.037$ and the elastic constants given in the text. Inset in (a) is the average magnetization for $L_z^{cf} = 0.3$ together with the experimental data of Ref. [10] rescaled so that $M^{avg}(0) = 0.35$.

$\psi_{a\sigma} = (1/\sqrt{2})(\psi_{1\sigma} + \psi_{2\sigma})$ and $\psi_{b\sigma} = (1/\sqrt{2})(\psi_{1\sigma} - \psi_{2\sigma})$, with $L_{a,b;\sigma} = \langle \psi_{a,b;\sigma} | L_i^z | \psi_{a,b;\sigma} \rangle = 0$ and eigenvalues $\epsilon_{a,b;\sigma} = \epsilon_{0\sigma} \pm \xi$. So in the absence of spin-orbit coupling, the average orbital angular momentum is quenched by the JT distortion and the doublet $\psi_{a,b;\sigma}$ is split by $2|\xi|$. The $T = 0$ energy is then given by

$$\frac{E}{N} = -3J_c SS' - \xi + \alpha \frac{\xi^2}{|\lambda|}, \tag{7}$$

where the final term is an elastic restoring potential and N is the number of Fe(II) or Fe(III) sites in each bimetallic layer. Since $\alpha > 0$, the $T = 0$ equilibrium value for ξ is $\xi(0) = |\lambda|/2\alpha > 0$.

Including the spin–orbit interaction $-|\lambda|\mathbf{L}_i \cdot \mathbf{S}_i$ and using the MF values $\epsilon_{1\sigma}$ and $\epsilon_{2\sigma}$ given by Eqs. (3) and (4), the eigenvalues of $\underline{H}_\sigma^{mix}$ are

$$\epsilon_{a\sigma} = \epsilon_{0\sigma} + t_\sigma, \tag{8}$$
$$\epsilon_{b\sigma} = \epsilon_{0\sigma} - t_\sigma, \tag{9}$$

where

$$t_\sigma = -\text{sgn}(\sigma)\sqrt{(\lambda L_z^{cf}\sigma)^2 + \xi^2}. \tag{10}$$

Hence, the doublet splitting $\delta \equiv 2|t_\sigma|$ is enhanced by the JT effect (strictly speaking, the pseudo-JT effect when $\epsilon_{1\sigma} \neq \epsilon_{2\sigma}$). Because there is no spin-orbit coupling when $\sigma = 0$, $t_0 = \xi$ and $L_{a0} = L_{b0} = 0$. Since $t_{-2} > 0$ and $\epsilon_{0,-2} < 0$, the lowest eigenvalue of $\underline{H}_\sigma^{mix}$ is $\epsilon_{b,-2}$.

For $\sigma \neq 0$, the spin-orbit coupling maintains a nonzero average orbital angular momentum $L_{a\sigma} = -L_{b\sigma}$ even in the presence of a JT distortion:

$$L_{a\sigma} = (L_z^{cf})^2 |\lambda|\sigma \frac{|\lambda| L_z^{cf}\sigma - t_\sigma}{(\lambda L_z^{cf}\sigma)^2 - |\lambda| L_z^{cf}\sigma t_\sigma + \xi^2}, \tag{11}$$

so that $L_{a\sigma} = L_{a,-\sigma}$. Since $\sigma t_\sigma < 0$, we see that $L_{a\sigma} \geqslant 0$. When $\xi \neq 0$, the JT distortion suppresses the average orbital angular momenta $L_{a\sigma} < L_z^{cf}$ for $\sigma = \pm 1$ and ± 2, as described in Ref. [8b].

With a correction to avoid double counting, the MF free energy can be written

$$\frac{F}{N} = -T \log \left\{ Z_{II} Z_{III} e^{3J_c M_S M_{S'}/4T} \right\}$$
$$+ \alpha|\lambda| \left\{ \left(\frac{\xi}{|\lambda|}\right)^2 + \gamma_3 \left(\frac{\xi}{|\lambda|}\right)^3 + \gamma_4 \left(\frac{\xi}{|\lambda|}\right)^4 \right\}, \tag{12}$$

where

$$Z_{II} = 2\sum_\sigma e^{-3J_c M_{S'}\sigma/2T} \cosh(t_\sigma/T), \tag{13}$$
$$Z_{III} = 2\sum_{\sigma'} e^{-3J_c M_S \sigma'/2T}. \tag{14}$$

The sums in the partition functions Z_{II} and Z_{III} are over $\sigma = 0, \pm 1, \pm 2$ and $\sigma' = \pm 1/2, \pm 3/2, \pm 5/2$. The second line in Eq. (12) corresponds to the elastic energy.

Breaking C_3 symmetry, a local JT distortion with $\pm \xi$ involves the displacement of an Fe(II) atom either into one of the three open hexagons or towards one of the three neighboring Fe(III) atoms. The former distortions are sketched in Fig. 1a. The $\gamma_3 (\xi/|\lambda|)^3$ term in Eq. (12) reflects the different energy costs for those two types of distortions. Thus, an anharmonic restoring potential arises quite naturally on the open honeycomb lattice. The sign of γ_3 does not affect any physical results and is chosen to be negative only for convenience so that the free energy is minimized when $\xi \geqslant 0$. Any fluctuations between the distorted atomic configurations are assumed slow compared to the electronic time scales.

It is simple to obtain the equilibrium values for M_S and $M_{S'}$ from the extremal conditions $\partial F/\partial M_S = \partial F/\partial M_{S'} = 0$:

$$M_S = \frac{4}{Z_{II}} \sum_\sigma \sigma e^{-3J_c M_{S'}\sigma/2T} \cosh(t_\sigma/T), \tag{15}$$
$$M_{S'} = 2S' B_{S'}(-3J_c M_S S'/2T), \tag{16}$$

where $B_{S'}(x)$ is the spin S' Brillouin function. Because the spin-orbit energy $-|\lambda|\mathbf{L}_i \cdot \mathbf{S}_i$ is treated exactly, M_L is not a variational parameter in the MF free energy and must be determined separately from the condition

$$M_L = -\frac{2}{Z_{II}} \sum_\sigma L_{a\sigma} e^{-3J_c M_{S'}\sigma/2T} \sinh(t_\sigma/T). \tag{17}$$

At $T = 0$, the $\sigma = -2$ term dominates in both the numerator and denominator of Eq. (17) and $M_L(0) = -L_{a2} = L_{b,-2} < 0$. Of course, the equilibrium value for the JT energy is obtained from the extremal condition $\partial F/\partial \xi = 0$.

3. Model results

The average magnetization and JT energy ξ are plotted versus temperature in Fig. 2a and b for $\alpha = 3.7$, $\gamma_3 = -1.9$, and $\gamma_4 = 1.1$.

As expected, the MC threshold $l_c \approx 0.282$ is enhanced by the JT distortion. When $L_z^{cf} < 0.260$, the JT distortion $\xi(T)$ persists down to $T = 0$. For $L_z^{cf} = 0$ (but still taking $\Delta > 0$), $\xi(0) \approx 0.842|\lambda| \approx 10.5$ meV and $T_{JT}^{(u)} \approx 0.578|\lambda|$. For $L_z^{cf} = 0.2$, the JT distortion would increase the splitting of the $\sigma = 2$ doublet from $4|\lambda|L_z^{cf} = 10$ meV to $2\sqrt{(2\lambda L_z^{cf})^2 + \xi^2} \approx 23$ meV.

When $L_z^{cf} \geqslant 0.260$, the JT distortion is quenched at $T = 0$ due to the strong orbital ordering. For $0.324 \geqslant L_z^{cf} \geqslant 0.260$, we obtain both lower and upper JT transitions, $T_{JT}^{(l)}$ and $T_{JT}^{(u)}$. Notice that ξ vanishes below $T_{JT}^{(l)}$ and is nonzero above $T_{JT}^{(l)}$. The temperature range $T_{JT}^{(u)} - T_{JT}^{(l)}$ decreases as L_z^{cf} increases and vanishes when $L_z^{cf} > 0.324$. We find that the JT transitions at $T_{JT}^{(u)}$ and $T_{JT}^{(l)}$ always bracket T_c. The first-order or discontinuous nature of the JT transitions at $T_{JT}^{(u)}$ and $T_{JT}^{(l)}$ is caused by the anharmonic term $\gamma_3(\xi/|\lambda|)^3$ in the free energy of Eq. (12).

Because the orbital contribution $M_L(T)$ to the Fe(II) moment drops as ξ jumps at the inverse JT transition, $T_{JT}^{(l)}$ is marked by a discontinuous increase in $M^{avg}(T)$. With decreasing L_z^{cf}, both the orbital contribution $M_L(T)$ and the magnitude of the change in $M^{avg}(T)$ become smaller. For $l_c < L_z^{cf} \leqslant 0.324$, the inverse JT transition is associated with a change in sign of $M^{avg}(T)$, as shown in the inset to Fig. 2a for $L_z^{cf} = 0.30$.

This inset shows the striking agreement between the theoretical prediction for $L_z^{cf} = 0.30$ and the measurements of Ref. [10] for A = N(n-C$_4$H$_9$)$_4$. So rather than indicating two compensation points, Ref. [10] provides compelling evidence for an inverse JT transition at $T_{JT}^{(l)} \approx 42$ K. According to Fig. 2b, a normal JT transition will be found at $T_{JT}^{(u)} \approx 70$ K. Indeed, recent X-ray measurements [14] on the same compound confirm that the hexagonal symmetry present at room temperature is absent in the monoclinic lattice below 60 K.

Measurements on several Fe(II)Fe(III) compounds [14,7] suggest that most MC compounds exhibit a small jump in the magnetization between T_c and T_{comp}. The predicted jumps in Fig. 2a are much too large to explain those measurements. X-ray diffraction studies [15] reveal that stacking faults in several compounds promote the coexistence of two phases: one with a six-layer repeat and the other with a two-layer repeat. The small magnetization jumps observed [14,7] in most MC compounds are likely caused by a mixture of those two stacking types. Indeed, a mixture of two phases, type 1 with $L_z^{cf} = 0.30$ (5% of the sample) and type 2 with $L_z^{cf} = 0.33$ (95% of the sample),[2] produces a small jump that is quite similar to the ones observed. The much larger jump found by Tang et al. [10] may be caused by the greater fraction of type 1 ($L_z^{cf} \approx 0.30$) stacking in their sample.

While there is no JT distortion ($\xi = 0$) when $\Delta < 0$, $\xi(T)$ remains nonzero down to $T = 0$ when $\Delta > 0$ and $L_z^{cf} < 0.260$. So our model predicts that normal bimetallic oxalates with $L_z^{cf} < 0.260$ will not exhibit a discontinuity in the magnetization, which may explain why such a jump has never been observed in a normal compound [7]. Nevertheless, normal Fe(II)Fe(III) compounds with $\Delta > 0$ (so that the doublet remains lowest in energy) should manifest a normal JT transition at $T_{JT}^{(u)} \approx 0.58|\lambda|$ or about 85 K.

But any non-C_3-symmetric cation like N(n-C$_4$H$_9$)$_4$ will also induce a permanent distortion of the hexagonal lattice. Depending on the size and shape of the cation, this distortion can be weakly-correlated or long-ranged. A non-C_3-symmetric potential can be included within our model by changing the off-diagonal terms in $\underline{H}_\sigma^{mix}$ from ξ to $\xi + \xi_0$. In the absence of spin–orbit coupling and a spontaneous JT distortion ξ, the doublet splitting δ is then $2\xi_0$. Since the anharmonic elastic potential proportional to ξ^3 fa-

vors $\xi > 0$, it acts to enhance the total distortion $|\xi + \xi_0|$ when $\xi_0 > 0$ and to suppress the total distortion when $\xi_0 < 0$. For any nonzero ξ_0, there is a spontaneous JT distortion $\xi(T) \neq 0$ at all temperatures due to the linear term of order $-\xi\xi_0/|\lambda|$ in the free energy.

As shown in Fig. 3 for $L_z^{cf} = 0.3$ and the elastic parameters given earlier, increasing ξ_0 for a fixed L_z^{cf} decreases $T_{JT}^{(l)}$ while keeping T_{comp} almost unchanged until $T_{JT}^{(l)} < T_{comp}$. When $\xi_0 > 0.047|\lambda| \approx 0.6$ meV, the spontaneous JT distortion ξ at $T = 0$ jumps to a value near $0.81|\lambda| \approx 10$ meV and the lower JT transition disappears. When $\xi_0 < -0.019|\lambda| \approx -0.2$ meV, the spontaneous JT distortion is eliminated but MC survives until $\xi_0 < -0.43|\lambda| \approx -5.4$ meV, as seen in the inset to Fig. 3a. Except in the narrow window $0 > \xi_0 > -0.019|\lambda|$, the permanent distortion ξ_0 and the electronic distortion ξ have the same sign. For either sign of ξ_0, MC is eliminated when the violation of C_3 symmetry and $|\xi_0|$ become sufficiently large.
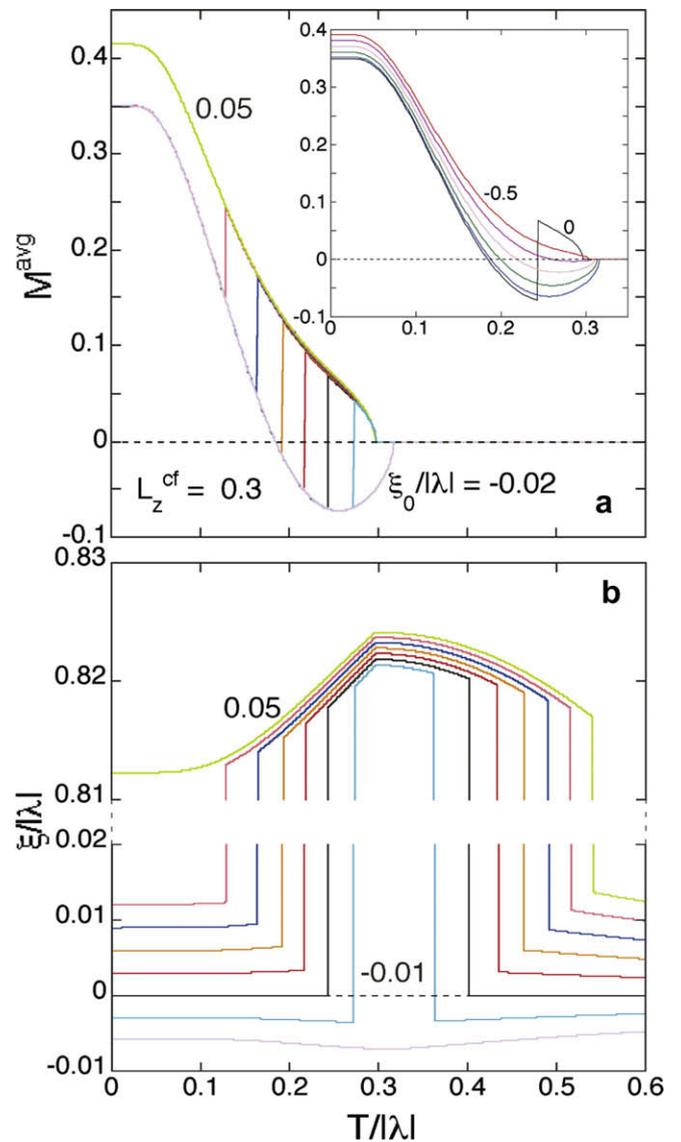

Fig. 3. (a) The average magnetization and (b) the JT mixing energy ξ normalized by $|\lambda|$ versus temperature $T/|\lambda|$ for several values of the permanent distortion $\xi_0/|\lambda|$ from −0.02 to 0.05 in increments of 0.01. Inset in (a) is the magnetization versus $T/|\lambda|$ for $\xi_0/|\lambda|$ between −0.5 and 0 in increments of 0.1. These plots use $L_z^{cf} = 0.3$, $J_c/|\lambda| = 0.037$ and the elastic constants given in the text.

[2] In a Mn(II)Fe(III) compound, Ref. [15a] reported a mixture of two stacking types with a faulting probability between 20% and 30%. In the Fe(II)Fe(III) family, MC compounds were found to be more monophasic.

Clearly, the electronic JT distortion ξ vanishes if the Fe(II) singlet lies below the doublet with $\Delta < 0$. So two conditions are required for C_3 symmetry to remain unbroken at $T = 0$. First, the cation itself must preserve C_3 symmetry so that there is no permanent distortion ξ_0. Second, either $\Delta < 0$ or if $\Delta > 0$, the average orbital angular momentum L_z^{cf} of the doublet must be sufficiently large to quench the spontaneous JT distortion ξ ($L_z^{cf} \geqslant 0.260$ in Fig. 2). Specific examples of symmetry breaking will be discussed in the next section.

4. First-principles calculations

In order to estimate the orders of magnitude of the spontaneous JT distortion ξ and the permanent distortion ξ_0, a series of first-principles calculations within the framework of density-functional theory (DFT) were performed. We employed the local spin-density approximation (SDA) in the plane-wave-pseudopotential approach with the PBE [16] exchange correlation functional as implemented in the Quantum-ESPRESSO package [17]. These calculations used Vanderbilt ultrasoft pseudopotentials [17–19] including, for the case of Fe [17,19], d electrons in the valence and non-linear core corrections. An energy cut-off of 600 eV was applied. Since the orbitals at the Fermi level are very localized in this ionic solid, we used a single **k**-point. Spin orbit coupling was not included. In order to stabilize the electronic density, the calculations were performed at an electronic temperature of 270 meV.

Predictions of the experimental electronic and magnetic structure in highly localized systems pose significant challenges for most approximations of DFT. Indeed, we find that the energy difference between ferromagnetic and antiferromagnetic configurations is below the resolution of our theory. Moreover, the charge-density wave observed experimentally (which results in inter-penetrated Fe(II) and Fe(III) networks) is not predicted to be the ground state. This discrepancy possibly signals the presence of strong self-interaction errors for the localized d orbitals [20]. The observed ferrimagnetic Fe(II)/Fe(III) ordering is stabilized by enforcing the net spin within each unit cell to equal 1/2.

Calculations were performed for several possible stackings (*ab*, *aab*, *abc*) of the bimetallic Fe(II)-Fe(III) layers with A = N(n-C$_3$H$_7$)$_4$ cations. As expected from the high degree of polymorphism and the low energy cost for stacking faults [15], the total energy differences between these three stackings were below the accuracy of our theory. Since the relative energy difference Δ between the doublet and singlet is quite sensitive to the stacking of the bimetallic planes, the angular momentum L_z^{cf} of the ground state may also depend on the stacking of the bimetallic planes.

The doublet splittings and the order of magnitude of the JT distortions were estimated by focusing on a single bimetallic layer with different cations A. Within hexagonal supercells, we studied the cations A = NH$_4$ (1) and N(n-C$_3$H$_7$)$_4$ (2). We also considered A = N(n-C$_3$H$_7$)$_4$ (3) in a non-hexagonal supercell.

(1) Because it is too small to stabilize the stacking of open honeycomb lattices, no oxalates actually contain the cation NH$_4$. However, calculations using this cation allow us to estimate the JT distortion in a C_3-symmetric environment. First, we relaxed the forces on all atoms while enforcing C_3 symmetry. The Fermi level for the majority band then lies at a doublet localized at the Fe(II) sites and occupied by a single electron. This configuration is consistent with our model, which requires the partial occupation of a doublet to explain the MC and the JT distortion. Second, the Fe(II) ion was displaced from the symmetric position on a grid of points **r**. From the *ab-initio* calculations, we extracted the total energy $E(\mathbf{r})$ of the configuration and the energy splitting $\delta(\mathbf{r})$ induced in the partially-occupied doublet. Because calculations where performed at an electronic temperature much larger than the splittings, both

electronic levels of the doublet have an equal occupation of 1/2. At this large electronic temperature, no JT electronic energy was gained and the symmetric point $\mathbf{r} = 0$ remained the position with minimum energy, as expected.

Nevertheless, the energy gain at $T = 0$ can be estimated as $E(\mathbf{r}) - \delta(\mathbf{r})/2$. This expression assumes that the total energy difference is given by the sum of the occupied eigenvalues at zero temperature and neglects a small change in the electronic density [21]. Within this approximation, we can estimate the Fe(II) position and doublet splitting at zero temperature. In the absence of the spin-orbit coupling, we find that the Fe(II) moves 0.03 Å (the nearest-neighbor Fe(II)–Fe(III) distance is about 5.4 Å) with an energy gain of 2 meV and a doublet spitting of 8 meV. This JT splitting is quite close to the spin–orbit coupling $|\lambda| L_z^{cf} S \approx 7.5$ meV with $L_z^{cf} = 0.3$.

(2) Because moderately-sized cations such as N(n-C$_3$H$_7$)$_4$ are themselves non-C_3-symmetric, they will break the C_3 symmetry of the crystal-field potential at the Fe(II) sites. While a N(n-C$_3$H$_7$)$_4$ isomer with three C$_3$H$_7$ radicals below the oxalate plane would preserve C_3 symmetry, the remaining propyl chain oriented towards the hexagonal hole in the oxalates plane must then break C_3 symmetry. This symmetry violation produces a crystal-field splitting $2\xi_0$ of the doublet and a permanent distortion of the open honeycomb lattice.

Calculations were performed in a hexagonal unit-cell containing a single A = N(n-C$_3$H$_7$)$_4$ cation with periodic boundary conditions, corresponding to to an ordered configuration where every N(n-C$_3$H$_7$)$_4$ cation is oriented in the same way. After relaxing the positions of the atoms, we obtained an intrinsic doublet splitting $2\xi_0$ of about 10 meV at an electronic temperature of 270 meV.

These calculations also indicate that the intrinsic distortion introduced by the cation will be increased at low temperature by the electronic energy gain of the Fe(II) JT distortion. So in the absence of spin-orbit coupling, the parameters ξ and ξ_0 of our model have the same sign for this cation.

(3) The molecule N(n-C$_3$H$_7$)$_4$ is just small enough to allow individual cations to rotate independently of each other. Hence, a uniform distortion of the crystal is possible. Such a uniform distortion of the open honeycomb structure has been observed in bimetallic oxalates with radical cations [22]. For an ordered arrangement of A = N(n-C$_3$H$_7$)$_4$ cations and allowing the supercell to break hexagonal symmetry, we obtain a doublet splitting $\delta \sim 20$ meV, which should increase to about 30 meV when the electronic temperature approaches zero.

By contrast, larger cations such as A = N(n-C$_4$H$_9$)$_4$ studied in Ref. [10] are unable to independently rotate within each unit cell. Locked into a highly-disordered configuration during synthesis, such cations will break the local C_3 symmetry around each Fe(II) ion but not the overall C_3 symmetry of the bimetallic planes. Since the spin–orbit coupling competes with the small, local lattice distortions, MC is still possible when the cations are large and disordered. This leads to an interesting conjecture: due to their ability to spatially order, smaller cations like N(n-C$_3$H$_7$)$_4$ may be more effective at enhancing the departure from C_3 symmetry and suppressing MC than larger cations like N(n-C$_4$H$_9$)$_4$.

5. Conclusion

The simple Hamiltonian introduced in Eq. (1) explains all of the important properties of Fe(II)Fe(III) bimetallic oxalates. It provides a natural explanation for the origin of the magnetic anisotropy on the Fe(II) sites due to the splitting of the $L = 2$ multiplet by the crystal-field potential. Unlike models [23,24] that rely on the inter-layer coupling, Eq. (1) explains the appearance of MC in compounds with large layer separations [6,7]. Because flipping the orbital angular momentum L_i^z requires an energy $2|\lambda| L_z^{cf} S \approx 175$ K

$\gg T_{comp}$, Eq. (1) explains the persistence of negative magnetization below T_{comp} in small fields. Due to the enhanced magnetic anisotropy and orbital moment, this model also explains why MC compounds have higher transition temperatures and Curie constants than normal compounds [6,7]. Finally, Eq. (1) explains the recently-observed jump [10] in the magnetization between T_{comp} and T_c, which is produced by an inverse JT transition.

Although these conclusions were based on a MF treatment of Eq. (1), Monte-Carlo calculations [25] have recently confirmed almost all of our earlier results [8], including the development of MC above a threshold value of L_z^{cf}. So we are confident that a more sophisticated analysis would also confirm our predictions for the lower and upper JT transitions.

Indeed, the robustness of the predicted inverse JT transition is easy to demonstrate. At high temperatures, fluctuations of the neighboring magnetic moments that are neglected within MF theory will also break the local C_3 symmetry and compete with the spin–orbit interaction. At low temperatures, however, magnetic fluctuations are suppressed and the spin-orbit interaction will act to restore C_3 symmetry. Therefore, the predicted inverse JT transition cannot be eliminated by magnetic fluctuations.

Our first-principles allow us to make more specific conclusions than are possible based on a phenomenological model alone. The calculations discussed in the previous section imply that large cations like $N(n\text{-}C_4H_9)_4$ induce a significant local distortion ξ_0 of the hexagonal lattice but are unable to reach an ordered ground state. On the other hand, smaller cations like $N(n\text{-}C_3H_7)_4$ can order at low temperatures. For an ordered configuration of $N(n\text{-}C_3H_7)_4$ cations with $|\xi_0| \approx 5$ meV (the value suggested by our first-principles results), the model results in Fig. 3 imply that an inverse JT transition will be absent and that, if present at all, MC will be rather weak with a high T_{comp}/T_c. Indeed, $N(n\text{-}C_3H_7)_4[Fe(II)Fe(III)ox_3]$ bimetallic oxalates [6] show no signs of a JT transition below T_c and a rather high compensation temperature of about $0.75T_c$.

With the spin–orbit coupling set to zero ($L_z^{cf} = 0$), the doublet splitting $\delta = 2\xi(0) \approx 21$ meV obtained using the model parameters of Fig. 2 is more than twice as large as that obtained from first-principles calculations in a C_3-symmetric environment. So it is likely that the organic cation $N(n\text{-}C_4H_9)_4$ plays a significant role in breaking the local C_3 symmetry and enhancing the doublet splitting. A more sophisticated description of the experimental measurements may be possible once additional information about the atomic structure becomes available.

Observation of the JT distortion between $T_{JT}^{(l)} \approx 42$ K and $T_{JT}^{(u)} \approx 70$ K in MC compounds would provide unambiguous support for the model of Eq. (1). We hope that this work will inspire systematic X-ray scattering measurements that will verify the predictions made in this paper, including the long-range ordering of small, non-C_3-symmetric cations in this important class of layered, molecule-based magnets.

References

[1] See for example: I.B. Bersuker, The Jahn–Teller Effect, Cambridge University Press, Cambridge, 2006. and references therein.
[2] J.B. Goodenough, Magnetism and the Chemical Bond, Interscience, New York, 1963.
[3] (a) M. Sorai, M. Nakano, Y. Miyazaki, Chem. Rev. 106 (2006) 976;
    (b) C. Beghidja, G. Rogez, J. Kortus, M. Wesolek, R. Welter, J. Am. Chem. Soc. 128 (2006) 3140;
    (c) J.A. Hatnean, R. Raturi, J. Lefebvre, D.B. Leznoff, G. Lawes, S.A. Johnson, J. Am. Chem. Soc. 128 (2006) 14992;
    (d) C.J. Milios, A. Vinslava, W. Wernsdorfer, A. Prescimone, P.A. Wood, S. Parsons, S.P. Perlepes, G. Christou, E.K. Brechin, J. Am. Chem. Soc. 129 (2007) 6547.
[4] H. Tamaki, Z.J. Zhong, N. Matsumoto, S. Kida, M. Koikawa, N. Achiwa, Y. Hashimoto, H. Õkawa, J. Am. Chem. Soc. 114 (1992) 6974.
[5] See the review: R. Clément, S. Decurtins, M. Gruselle, C. Train, Mon. für Chem. 117 (2003) 117.
[6] (a) C. Mathoniére, S.G. Carling, P. Day, J. Chem. Soc., Chem. Commun. (1994) 1551;
    (b) C. Mathonière, C.J. Nuttall, S.G. Carling, P. Day, Inorg. Chem. 35 (1996) 1201.
[7] C.J. Nuttall, P. Day, Chem. Mater. 10 (1998) 3050.
[8] (a) R.S. Fishman, F.A. Reboredo, Phys. Rev. Lett. 99 (2007) 217203;
    (b) R.S. Fishman, F.A. Reboredo, Phys. Rev. B 77 (2008) 144421.
[9] R.S. Fishman, S. Okamoto, F.A. Reboredo, Phys. Rev. Lett. 101 (2008) 116402.
[10] G. Tang, Y. He, F. Liang, S. Li, Y. Huang, Physica B 392 (2007) 337.
[11] E.I. Stiefel, G.F. Brown, Inorg. Chem. 11 (1972) 436.
[12] B. Bleaney, K.W.H. Stevens, Rep. Prog. Phys. 16 (1953) 108.
[13] P. Reis, R.S. Fishman, F.A. Reboredo, J. Moreno, Phys. Rev. B 77 (2008) 174433.
[14] I.D. Watts, S.G. Carling, P. Day, D. Visser, J. Phys. Chem. Solids 66 (2005) 932.
[15] (a) C.J. Nuttall, P. Day, J. Solid State Chem. 147 (1999) 3;
    (b) N.S. Ovanesyan, V.D. Makhaev, S.M. Aldoshin, P. Gredin, K. Boubekeur, C. Train, M. Gruselle, Dalton Trans. 18 (2005) 3101.
[16] J.P. Perdew, K. Burke, M. Ernzerhof, Phys. Rev. Lett. 77 (1996) 3865.
[17] S. Baroni, A. Dal Corso, S. deGironocli, P. Giannozzi, <http://www.pwscf.org>.
[18] D. Vanderbilt, Phys. Rev. B 41 (1990) 7892.
[19] A.M. Rappe, K.M. Rabe, E. Kaxiras, J.D. Joannopoulos, Phys. Rev. B 41 (1990) 1227.
[20] J.P. Perdew, A. Zunger, Phys. Rev. B 23 (1981) 5048.
[21] See Eq. (17) in: J. Ihm, A. Zunger, M. Cohen, J. Phys. C 12 (1979) 4409.
[22] (a) M. Clemente-León, E. Coronado, J.R. Galán-Mascarós, C.J. Gómez-García, Chem. Commun. (1997) 1727;
    (b) E. Coronado, J.R. Galán-Mascarós, C.J. Gómez-García, J. Ensling, P. Gütlich, Chem. Eur. J. 6 (2000) 552.
[23] Y. Nakamura, J. Phys.: Condens. Matter 12 (2000) 4067.
[24] Y. Nakamura, Phys. Rev. B 62 (2000) 11742.
[25] P. Henelius, R.S. Fishman, Phys. Rev. B 78 (2008) 214405.